Polym. Bull. (2011) 67:937–950
DOI 10.1007/s00289-010-0426-3

ORIGINAL PAPER

Intriguing liquid crystalline behavior of liquid crystalline polyrotaxane containing azobenzene mesogens

Tianhui Hu · Helou Xie · Li Chen · Sheng Chen · Hailiang Zhang

Received: 24 December 2009 / Revised: 23 September 2010 / Accepted: 12 December 2010 /
Published online: 31 December 2010

Abstract A series of liquid crystalline polyrotaxanes containing azobenzene mesogenic moieties (AzoPR) with different length of spacer were synthesized, and the relationship between the spacer length and the liquid crystalline behavior was investigated. The molecular characterization of the AzoPR was performed with ^{1}H NMR, FT-IR, and gel permeation chromatography. The thermal stability was investigated via thermogravimetric analysis. Their phase structures and liquid crystalline properties were studied by differential scanning calorimetry, polarized optical microscopy and wide-angle X-ray diffraction. The experimental results suggested that AzoPR with spacer length of 2 and 4 failed to show the liquid crystalline behavior, and AzoPR with spacer length of 6 showed the columnar nematic phase. However, when the spacer length increases to 11, the columnar nematic phase formed, meanwhile, the liquid crystalline domains with high ordered structure were developed by azobenzene mesogens.

Keywords Liquid crystal · Polyrotaxane · Spacer length

Introduction

During the last three decades, synthesis and study of the phase structures and transitions of various thermotropic liquid crystalline polymers (LCPs) have been one of the most important topics in polymer chemistry and physics [1]. In particular, LCPs containing azobenzene chromophores are distinguished due to their diverse potential applications, such as actuators, optical switches, and optical data storage [2–7],

T. Hu · H. Xie · L. Chen · S. Chen · H. Zhang (✉)
Key Laboratory of Polymeric Materials and Application Technology of Hunan Province, Key Laboratory of Advanced Functional Polymer Materials of Colleges and Universities of Hunan Province, College of Chemistry, Xiangtan University, Xiangtan, Hunan 411105, People's Republic of China
e-mail: hailiangzhang@xtu.edu.cn

because azobenzene chromophores can undergo reversible photoisomerization between the stretched *trans* and the bent *cis* isomers when they are exposed to certain wavelengths or heating, which lead to considerable changes in their molecular shape, size, and dipole moments as well as optical properties [8, 9].

On the other hand, nanometer-scaled supramolecular assemblies constructed by the simple inclusion complexation of cyclodextrins (CDs) with organic molecules represent a very active topic of science and technology due to their potential to serve as molecular devices, molecular machines, and functional materials [10–14]. Among them, CD-based polyrotaxanes (PRs) as new polymeric materials have attracted more and more attention. PRs are one of the supramolecular polymers in which a number of cyclic molecules are threaded onto a linear polymer chain and are mechanically interlocked in the polymer chain by bulky end groups [15–24]. The most characteristic feature of PRs is that each macrocycle slides rotate on the polymer chain. Based on this feature, many fascinating molecular materials have been reported [25–30]. Especially, PR from α-CD and PEG has been studied most intensively because of the facility in synthesis as well as the biocompatibility of the components [10, 18, 21, 31]. Besides, α-CD moiety of PR is very convenient for modification by a variety of functional groups because it has 18 hydroxyl groups. Recently, Kidowaki et al. [16] has reported the first synthesis of liquid crystalline PR and investigated the liquid crystalline behavior of this novel side chain LCPs with mobile mesogens along the polymer main chain that can rotate around the chain. However, as we know the relationship between the spacer length and the formation of liquid crystalline phase has hardly been reported, moreover, there is no investigation about the thermotropic behavior of the liquid crystalline PR containing azobenzene mesogenic moieties (AzoPR).

In this article, we report the synthesis of a series of AzoPR, and investigate the thermotropic behavior dependence of the spacer length. The molecular model of AzoPR with spacer length of 11 is showed in Fig. 1. The molecular characterizations of the resultant polymers AzoPR-*m*, where *m* represents the length of spacer, were performed with ^{1}H NMR, FT-IR, gel permeation chromatography (GPC), and thermogravimetric analysis (TGA). Their phase transitions and liquid-crystalline behaviors of these polymers are investigated by differential scanning calorimetry (DSC), polarized optical microscopy (POM), and wide-angle X-ray diffraction (WAXD).

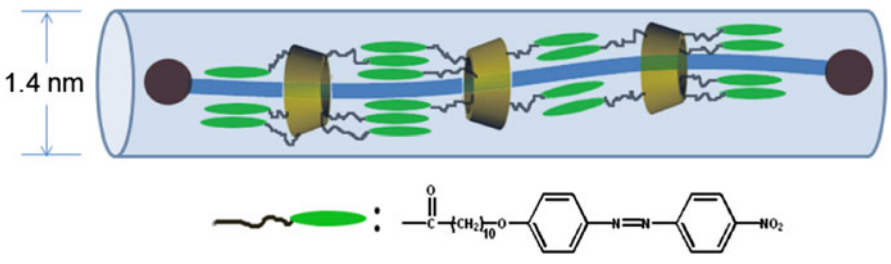

Fig. 1 The molecular model of AzoPR-11

Experimental section

Materials

All the materials used in this study were commercial samples and were used as supplied, unless otherwise stated. The PR used in this study was prepared from α-CD, poly(ethylene glycol) of average molecular weight 8000 and 3,5-dimethylphenol, according to the literature [18]. The number of α-CD in the PR was estimated to be ca. 25 from the ^{1}H NMR signals, which corresponded to 27% coverage of the PEG chain by α-CDs, assuming that one α-CD molecule could perfectly cover two PEG monomer units. Ethyl bromoacetate (98%, Alfa Aesar), ethyl 4-bromobutyrate (98%, Alfa Aesar), ethyl 6-bromohexanoate (99%, Alfa Aesar), 3,5-dimethylphenol (98%, Alfa Aesar), *p*-nitroaniline (Tianjin Guangfu Fine Chemical Research Institute), 11-bromoundecanoic acid (Taiyuan Zhonglian Zenong Chemical Industry Co., Ltd.) were used as received.

Synthesis of the intermediates and AzoPR

The chemical structure and synthesis route of the azobenzene mesogens are illustrated in Scheme 1. The experimental details are described as follows.

4-Nitro-4′-hydroxy azobenzene

The diazonium coupling reaction was employed to prepare 4-nitro-4′-hydroxy azobenzene according to the literature [32]. A solution of sodium nitrite (24.8 g, 0.36 mol) in water was added dropwise with stirring to a solution of *p*-nitroaniline (49.7 g, 0.36 mol) in 300 mL distilled water and 90 mL concentrated HCl in an ice bath. After 30 min stirring, phenol (33.8 g, 0.36 mol) and NaOH (36 g, 0.9 mol) dissolved in 100 mL water was added with vigorous stirring at 0 °C. The precipitate

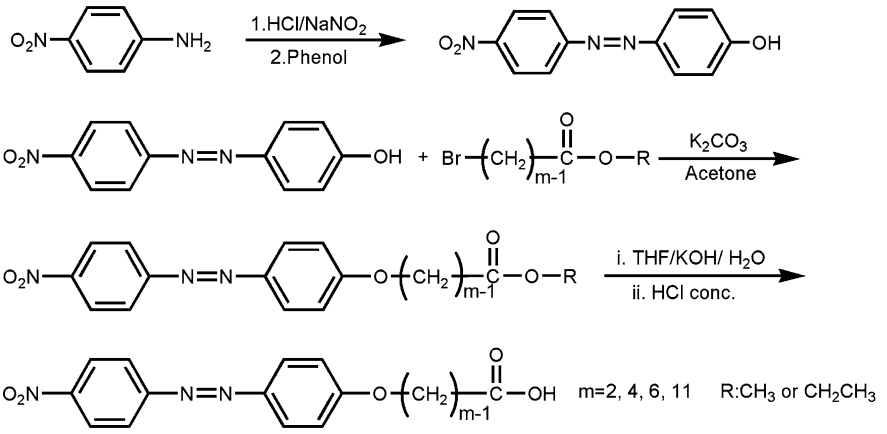

Scheme 1 The synthesis route of azobenzene mesogens

formed was filtered and washed repeatedly with water to remove any remaining reactants. The product was recrystallized from ethanol/water (1:3) and dried under vacuum. Yield: 82%. ^{1}H NMR (400 MHz, $CDCl_3$-d, ppm): 8.39 (d, $J = 10.0$ Hz, 2H, Ar–H), 7.96 (m, 4H, Ar–H), 6.98 (d, $J = 9.3$ Hz, 2H, Ar–H), 5.17 (br-s, 1H, –OH).

Ethyl 4-(4-nitroazobenzene-4′-yloxy) butyrate (N4E)

Ethyl 4-bromobutyrate (16.0 g, 0.082 mol), 4-nitro-4′-hydroxy azobenzene (13.3 g, 0.055 mol) and anhydrous potassium carbonate (38.0 g, 0.275 mol) were stirred in acetone (200 mL) in a flask under nitrogen atmosphere under reflux for 48 h. Subsequently, the solution was precipitated into cold water and collected by vacuum filtration. The crude product was purified by recrystallization from acetone, and then separated through a silicon column using CH_2Cl_2 as the eluent. The first ingredient was collected. By removing the solvent with rotate vaporizing apparatus, the product, N4E as yellow crystals was obtained. Yield: 79%, yellow crystals. ^{1}H NMR (400 MHz, $CDCl_3$-d, ppm): 8.36 (d, $J = 8.2$ Hz, 2H, Ar–H), 7.97 (m, 4H, Ar–H), 7.02 (d, $J = 9.8$ Hz,2H, Ar–H), 4.16 (m, 4H, –CH_2–), 2.55 (t, 2H, –CH_2–), 2.16 (t, 2H, –CH_2–), 1.27 (t, 3H, –CH_3).

4-(4-Nitroazobenzene-4′-yloxy) butyric acid (N4C)

The N4E (15.0 g, 0.042 mol) and potassium hydroxide (23.5 g, 0.420 mol) were stirred in 200 mL THF/H_2O (1:1) for 10 h under reflux in a flask under nitrogen atmosphere. The resultant slurry was poured into water (500 mL) and then neutralized with concentrated HCl. The yellow precipitate was filtered off, washed with water, and dried under vacuum. Recrystallization from ethanol (700 mL) provided N4C as yellow crystals. Yield: 88%, yellow crystals. ^{1}H NMR (400 MHz, DMSO-d_6, ppm): 12.19 (s, 1H, –COOH), 8.41 (d, $J = 9.0$ Hz, 2H, Ar–H), 8.02 (m, 4H, Ar–H), 7.18 (d, $J = 9.0$ Hz, 2H, Ar–H), 4.12 (t, 2H, –OCH_2–), 2.41 (t, 2H, –CH_2–), 1.96 (m, 2H, –CH_2–). ^{13}C NMR: 174.65 (C=O), 162.95 (aromatic C–O), 156.06 (aromatic C–N), 148.37 (aromatic C–NO_2), 147.04 (aromatic C–N), 125.87, 125.41 (aromatic C), 123.84 (aromatic C), 115.95 (aromatic C), 67.74 (–OCH_2–), 30.63 (–CH_2–C=O), 24.55 (–CH_2–). Anal. Calcd for $C_{16}H_{15}N_3O_5$: C, 58.36; N, 12.76; H, 4.59; Found: C, 58.28; N, 12.70; H, 4.48. Melting point: 185–187 °C.

Ethyl 2-(4-nitroazobenzene-4′-yloxy) acetate (N2E)

Compound N2E was similarly synthesized as N4E by using ethyl bromoacetate. Yield: 83%, yellow crystals. ^{1}H NMR (400 MHz, $CDCl_3$-d, ppm): 8.35 (d, $J = 9.1$ Hz, 2H, Ar–H), 7.96 (m, 4H, Ar–H), 7.04 (d, $J = 8.8$ Hz, 2H, Ar–H), 4.74 (s, 2H, –CH_2–), 4.31 (t, 2H, –$COOCH_2$–), 1.30 (t, 3H, –CH_3).

2-(4-Nitroazobenzene-4′-yloxy) acetic acid (N2C)

Compound N2C was similarly synthesized as N4C. Yield: 85%, yellow crystals. ^{1}H NMR (400 MHz, DMSO-d_6, ppm): 13.20(s, 1H, –COOH), 8.41 (d, $J = 9.1$ Hz,

2H, Ar–H), 8.02 (m, 4H, Ar–H), 7.18 (d, $J = 8.8$ Hz, 2H, Ar–H), 4.84 (s, 2H, $–CH_2–$). ^{13}C NMR: 170.35 (C=O), 162.13 (aromatic C–O), 155.84 (aromatic C–N), 148.59 (aromatic C–NO_2), 146.90 (aromatic C–N), 125.74, 125.49 (aromatic C), 123.65 (aromatic C), 115.88 (aromatic C), 65.74 ($–CH_2–$). Anal. Calcd for $C_{14}H_{11}N_3O_5$: C, 55.82; N, 13.95; H, 3.68; Found: C, 55.71; N, 13.86; H, 3.59. Melting point: 251–252 °C.

Ethyl 6-(4-Nitroazobenzene-4′-yloxy) hexanoate (N6E)

Compound N6E was similarly synthesized as N4E by using ethyl 6-bromohexanoate. Yield: 78%, yellow crystals. ^1H NMR (400 MHz, $CDCl_3$-d, ppm): 8.35 (d, $J = 8.8$ Hz,2H, Ar–H), 7.96 (m, 4H, Ar–H), 6.98 (d, $J = 8.7$ Hz, 2H, Ar–H), 4.06 (t, 2H, $–OCH_2–$), 4.15 (t, 2H, $–COOCH_2–$), 2.35 (t, 2H, $–CH_2COO–$), 1.50–1.87 (m, 6H, $–CH_2–$), 1.26 (t, 3H, $–CH_3$).

6-(4-Nitroazobenzene-4′-yloxy) hexanoic acid (N6C)

Compound N6C was similarly synthesized as N4C. Yield: 86%, yellow crystals. ^1H NMR (400 MHz, DMSO-d_6, ppm): 12.0 (s, 1H, –COOH), 8.39 (d, $J = 8.8$ Hz, 2H, Ar–H), 8.02 (m, 4H, Ar–H), 7.17 (d, $J = 8.9$ Hz, 2H, Ar–H), 4.10 (t, 2H, $–OCH_2–$), 2.22 (t, 2H, $–CH_2–$), 1.42–1.78 (m, 6H, $–CH_2–$). ^{13}C NMR: 174.85 (C=O), 162.88 (aromatic C–O), 155.99 (aromatic C–N), 148.37 (aromatic C–NO_2), 146.84 (aromatic C–N), 125.90, 125.47 (aromatic C), 123.59 (aromatic C), 115.95 (aromatic C), 68.54 ($–OCH_2–$), 33.97 ($–CH_2–C=O$), 28.75 ($–CH_2–$), 25.54 ($–CH_2–$), 24.72 ($–CH_2–$). Anal. Calcd for $C_{18}H_{19}N_3O_5$: C, 60.50; N, 11.76; H, 5.36; Found: C, 60.41; N, 11.65; H, 5.29. Melting point: 166–168 °C.

Methyl 11-(4-nitroazobenzene-4′-yloxy) undecanoate (N11M)

Compound N11M was similarly synthesized as N4E starting from 11-bromoundecanoic acid [33]. Yield: 85%, yellow crystals. ^1H NMR (400 MHz, $CDCl_3$-d, ppm): 8.34 (d, $J = 9.0$ Hz, 2H, Ar–H), 7.98 (m, 4H, Ar–H), 7.04 (d, $J = 9.0$ Hz, 2H, Ar–H), 4.06 (t, 2H, $–OCH_2–$), 3.67 (s, 3H, $–CH_3$), 2.32 (t, 2H, $–CH_2COO–$), 1.31–1.85 (m, 16H, $–CH_2–$). ^{13}C NMR: 174.25 (C=O), 163.08 (aromatic C–O), 156.20 (aromatic C–N), 148.24 (aromatic C–NO_2), 146.84 (aromatic C–N), 125.44 (aromatic C), 124.57 (aromatic C), 123.03 (aromatic C), 114.88 (aromatic C), 68.68 ($–OCH_2–$), 51.29 ($–CH_3$), 33.91 ($–CH_2–C=O$), 29.43($–CH_2–$), 29.31($–CH_2–$), 29.28 ($–CH_2–$), 29.18 ($–CH_2–$), 29.13 ($–CH_2–$), 29.11 ($–CH_2–$), 25.97 ($–CH_2–$), 24.93 ($–CH_2–$). Anal. Calcd for $C_{24}H_{31}N_3O_5$: C, 65.29; N, 9.52; H, 7.08; Found: C, 65.18; N, 9.43; H, 6.97. Melting point: 131–132 °C.

11-(4-Nitroazobenzene-4′-yloxy) undecanoic acid (N11C)

Compound N11C was similarly synthesized as N4C. Yield: 80%, yellow crystals. ^1H NMR (400 MHz, DMSO-d_6, ppm): 11.70 (s, 1H, –COOH), 8.42 (d, $J = 8.9$ Hz, 2H, Ar–H), 8.03 (m, 4H, Ar–H), 7.18 (d, $J = 9.0$ Hz, 2H, Ar–H), 4.12 (t, 2H,

–OCH_2–), 2.18 (t, 2H, –CH_2–), 1.27–1.78 (m, 16H, –CH_2–). ^{13}C NMR: 174.85 (C=O), 163.35 (aromatic C–O), 156.01 (aromatic C–N), 148.32 (aromatic C–NO_2), 146.80 (aromatic C–N), 125.94, 125.52 (aromatic C), 123.61 (aromatic C), 115.82 (aromatic C), 68.68 (–OCH_2–), 33.91 (–CH_2–C=O), 29.37 (–CH_2–), 29.31 (–CH_2–), 29.23 (–CH_2–), 29.17 (–CH_2–), 29.11 (–CH_2–), 29.02 (–CH_2–), 25.85 (–CH_2–), 24.94 (–CH_2–). Anal. Calcd for $C_{23}H_{29}N_3O_5$: C, 64.62; N, 9.83; H, 6.84; Found: C, 64.53; N, 9.72; H, 6.75. Melting point: 113–114 °C.

4-(4-Nitroazobenzene-4′-yloxy) butyryl chloride

The N4C (0.46 g, 1.41 mmol) was added to thionyl chloride (100 mL) in an ice bath and stirred for 15 h at room temperature in a flask under nitrogen atmosphere, giving a clear yellow solution. This solution was then gently heated to 50 °C for 60 min to expel any remaining gases from solution. The excess thionyl chloride was then removed under the reduced pressure, and the oily residue coevaporated several times with dry petrol ether. The acid chloride was then used in the next step without further purification.

Preparation of the AzoPR

A typical synthesis procedure for AzoPR is described here for sample AzoPR-4 in Table 1. PR (0.1 g), dried under vacuum at 80 °C for 1 h, was dissolved in 5 mL of dry N,N′-dimethylacetamide (DMA) with 8% lithium chloride (LiCl). To the solution, triethylamine (0.86 g, 8.48 mmol) and a dry DMA solution of the above-prepared acid chloride (2.0 equiv to hydroxyl groups of PR) was slowly added under nitrogen atmosphere in an ice bath and then stirred for 24 h at room temperature. The reaction mixture was poured into excess water, and the precipitate was collected by filtration. The obtained solid was dissolved in DMA and precipitated from methanol and ethanol several times and then collected by

Table 1 GPC, DSC, and TGA results and thermotropic properties of AzoPR

Samples	Mn[a] ($\times 10^{-4}$/g/mol)	Mw/Mn[a]	DS[b]	Phase transitions (°C) and corresponding enthalpy changes under cooling (J/g)[c]	$T^{d}_{d,N2}$ (°C)	$T^{e}_{d,air}$ (°C)
AzoPR-2	9.80	1.29	5.96	Tg131	327	318
AzoPR-4	8.62	1.36	5.88	Tg105	320	315
AzoPR-6	10.98	1.32	6.15	Tg72N197 (0.28)I	332	325
AzoPR-11			6.03	Tg47K153 (0.21)	331	324

[a] Obtained from PL-GPC120 instrument, linear PS as standards

[b] DS was determined by ^{1}H NMR

[c] Phase transitions and corresponding enthalpy changes was evaluated by DSC at a rate of 10 °C/min under cooling. K represents the complex phase of AzoPR-11 as explained hereinafter

[d,e] The temperature at which 5% weight loss of the sample was reached from TGA under nitrogen atmosphere and air atmosphere, respectively

centrifugation. The precipitate was then soxhlet-extracted with methanol and dried under vacuum.

Measurements

^{1}H NMR spectra were recorded on a BRUKER ARX400 MHz spectrometer with tetramethylsilane (TMS) as the internal standard at room temperature in chloroform-d ($CDCl_3$) or dimethyl sulfoxide-d6 (DMSO-d6). FT-IR spectra in KBr pellets were recorded on a PE Spectrum One FT-IR spectrophotometer.

The GPC measurements were performed on a PL-GPC120 setup equipped with a column set consisting of two PL gel 5 μm MIXED-D columns (7.5 × 300 mm, effective molecular weight range of 0.2–400.0 kg/mol) using *N*,*N*′-dimethyl formamide (DMF) that contained 0.01 M LiBr as the eluent at 80 °C at a flow rate of 1.0 mL/min. Narrowly distributed polystyrene standards in the molecular weight range of 0.5–7500.0 kg/mol (PSS, Mainz, Germany) were utilized for calibration.

The TGA was performed on a TGA Q50 instrument at a heating rate of 20 °C/min under nitrogen atmosphere and air atmosphere, respectively.

The thermal transitions of AzoPR were detected using DSC (TA-Q10). The temperature and heat flow were calibrated using standard materials (indium and zinc) at cooling and heating rate of 10 °C/min. Samples with a typical mass of 3–10 mg were encapsulated in sealed aluminum pans. The DSC thermal diagrams were recorded at 10 °C/min during the second heating process.

The LC texture of the polymers was examined under POM (Leica DM-LM-P) coupled with a Mettler-Toledo hot stage (FP82HT). Powder sample was placed between two glass slides and the photographs were obtained during the second heating.

The WAXD powder experiments were performed on a Philips X'Pert Pro diffractometer with a 3 kW ceramic tube as the X-ray source (Cu KR) and an X'celerator detector. The sample stage was set horizontally. The reflection peak positions were calibrated with silicon powder ($2\theta > 15°$) and silver behenate ($2\theta < 10°$). Background scattering was recorded and subtracted from the sample patterns. A temperature control unit (Paar Physica TCU 100) in conjunction with the diffractometer was utilized to study the structure evolutions as a function of temperature.

Results and discussion

Synthesis and characterization of intermediates and AzoPR

As shown by Scheme 1, N4C was successfully synthesized through a multistep reactions route according to a procedure described in the literature [33]. First, 4-nitro-4′-hydroxy azobenzene was prepared by reaction of *p*-nitroaniline and phenol through the classical diazo-reaction. Then, the obtained 4-nitro-4′-hydroxy

azobenzene was refluxed with ethyl 4-bromobutyrate in acetone in the presence of anhydrous potassium carbonate to give N4E. Finally, N4C was obtained by the saponification of N4E in THF and water with potassium hydroxide. The purity and chemical structure were confirmed by thin-layer chromatography and ^{1}H NMR. The acids with shorter spacer were synthesized according to the same method using ethyl bromoacetate, ethyl 6-bromohexanoate, and 11-bromoundecanoic acid.

Polyrotaxane comprised of PEG (average molecular weight 8000) and α-CD was prepared according to the method [18]. The number of α-CDs in a single PR is estimated at ca. 25 from the ^{1}H NMR signals, which corresponds to 27% coverage of the PEG chains with α-CDs. As we all know, the modification of PR is severely limited to the lack of good solvent because it is insoluble in common solvent except DMSO and aqueous sodium hydroxide (NaOH). Recently, ARAKI and ITO have reported an effective solvent system of dimethylacetamide/lithium chloride (DMA/LiCl) for PR modification [34].

In this study, the esterification of PR with acid chloride of azobenzene was conducted using triethylamine as catalyst in DMA containing 8% LiCl solution homogeneously. To examine the influence of spacer length on the thermotropic behavior of AzoPR, a series of samples were prepared.

Figure 2 shows the FT-IR spectra of AzoPR and the unmodified PR. The most typical peak is observed for all AzoPR at about 1740 cm^{-1}, assigned to the stretching of the esters group. Another significant peak is the stretching vibration of methylene at 2925 and 2853 cm^{-1}, this peak enhanced accompanied with the increase of the spacer length. These signals directly demonstrate that azobenzene-based mesogens are successfully grafted on the main chain of PR. Nevertheless, the broad peak at about 3000–3700 cm^{-1} is attributed to the residual hydroxyl of the cyclodextrin in the spectra of AzoPR.

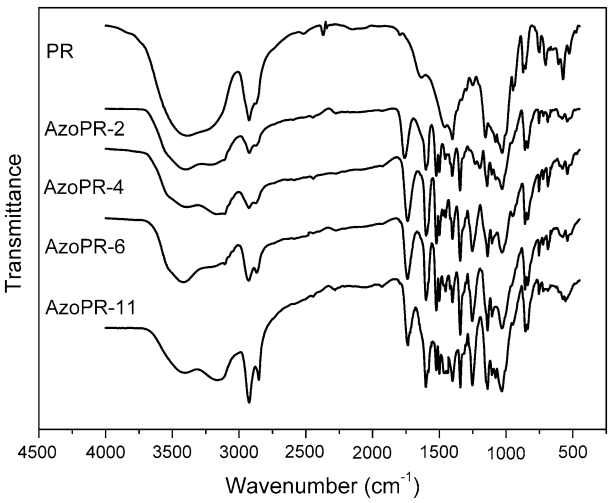

Fig. 2 FT-IR spectra of PR and the corresponding AzoPR

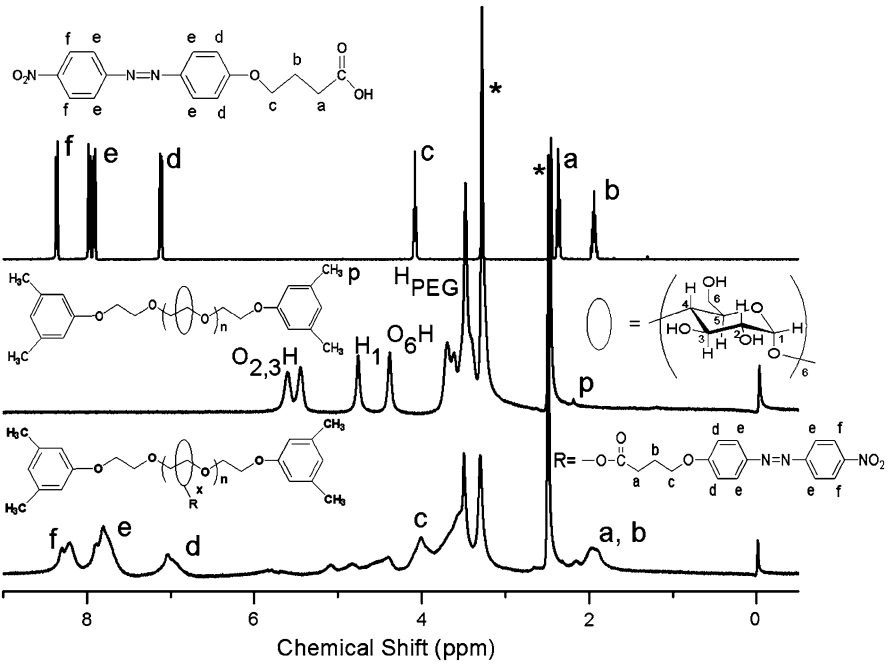

Fig. 3 ^{1}H NMR spectra of N4C (*upper*), PR (*middle*), and AzoPR-4 (*bottom*) in DMSO-d_6

The chemical structure of AzoPR is confirmed by ^{1}H NMR in DMSO-d_6, and all the chemical shifts of the polymers are consistent with the samples. Herein, to illuminate concretely, ^{1}H NMR spectra of N4C, unmodified PR and AzoPR-4 are shown in Fig. 3 as example. From Fig. 3, it is evidence that the chemical shifts of the PR are broadened and weakened after modification. However, peaks in the region of 6.7–8.5 ppm originating from the phenyl rings and the peaks at 1.7–2.1 ppm for aliphatic hydrogen of side chain are distinctly observed. These results coincide well with the result of FT-IR. The degree of substitution (DS), that is, the average number of azobenzene mesogen attached to the per α-CD, can be calculated from the respective ^{1}H NMR spectra by comparing the integrations between the regions at 6.7–8.5 ppm (phenyl rings) and at 4.3–6.0 ppm (residual hydroxyl group and H_1 of the cyclodextrin) in DMSO-d_6, and this result is also confirmed using TMS as internal standard for integration. The results are showed in Table 1.

The GPC was performed to determine the apparent molecular weight (MW) and molecular weight distribution of the polymers. The apparent MW is showed in Table 1. The GPC data of AzoPR-11 can not be obtained owing to the poor solubility except for DMSO. From the data in Table 1, it is evident that all the AzoPR has the similar MW and molecular weight distribution; on the other hand, the DS of the samples is also almost the same, so we further study the effect of spacer length on the liquid crystalline behavior.

Thermal transitions behavior of AzoPR

Before investigating the thermotropic behavior of the polymers, we first examined their thermal stabilities via TGA under nitrogen and air atmosphere, respectively. Figure 4 shows the TGA curves of free α-CD, unmodified PR, and AzoPR with different spacer length under nitrogen atmosphere. It can be found that PR undergoes two-step thermal degradation corresponding to the degradation of α-CD and PEG chain in the PR [35]. The result also reveals that AzoPR starts to decompose earlier after modification compared with unmodified PR. When the atmosphere is changed from nitrogen to air, the thermal decomposition occurred earlier.

Thermal transition behavior of the resultant polymers is studied by DSC. The DSC thermal diagrams were recorded at 10 °C/min during the second heating process, of which the DSC traces are showed in Fig. 5. It can be found that the glass transition temperatures decreases with the increase of spacer length, owing to the fact that long spacer serve as "diluents" and increase the free volume [36, 37]. Compared with AzoPR-2 and AzoPR-4, an endothermic peak appears for AzoPR-6 and AzoPR-11 besides the glass transition, illuminating that an ordered structure is formed above the temperature of glass transition. Moreover, we observed an unexpected problem that the degradation came earlier after the endothermic transition finished during the heating procedure, indicating that the cyclodextrin on the AzoPR started to degrade. However, TGA can not reflect this delicate transformation, and the reason may be that the covalent bond of cyclodextrin is broken without the loss of weight at higher temperature.

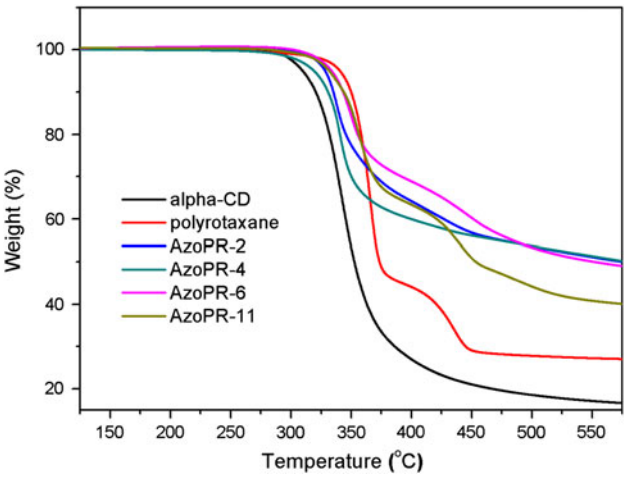

Fig. 4 TGA curves of α-CD, PR and the corresponding AzoPR, acquired under nitrogen atmosphere

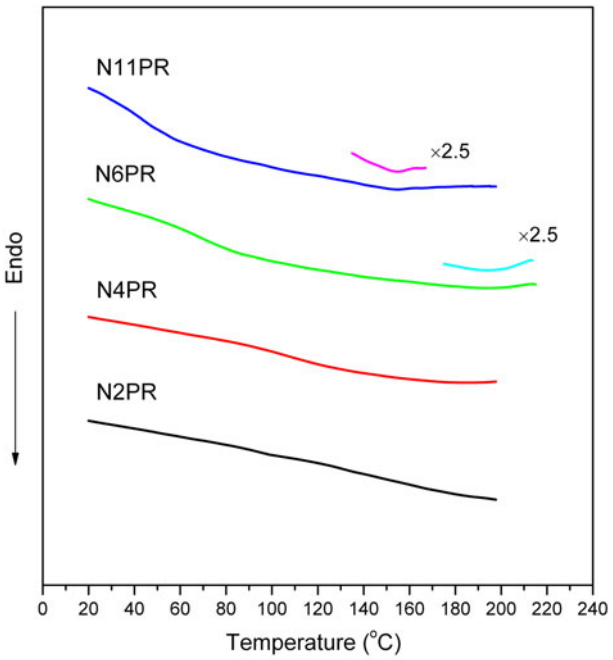

Fig. 5 DSC thermal diagrams of AzoPR during the second heating at a rate of 10 °C/min

Phase structures of AzoPR

The nature of mesophases formed by present polymers was studied by observing optical textures on a polarizing optical microscope and their X-ray analysis. Birefringence can not be obtained for AzoPR-2 and AzoPR-4 during the heating and corresponding cooling process from POM, indicating that the liquid crystalline phase can not be formed due to the short spacer. AzoPR-6 and AzoPR-11 revealed optical textures without any specific feature (as showed in Fig. 6a, b), by which the morphology of the mesophases could not be clearly identified, that is, observed optical textures did not provide us with any clear clues regarding the nature of their mesophases.

The structure of the liquid crystalline phase was further studied with WAXD. Before collecting the signals, the samples were heated to 120 °C at a rate of 10 °C/min and kept for 10 min. Figure 7 shows the WAXD patterns of the treated AzoPR-6 and AzoPR-11. As showed in Fig. 7, there are two diffraction peaks for AzoPR-6, one at the low angle region about $2\theta = 6.3°$ (14.0 Å), and the other at the wide angle region at about $2\theta = 20.4°$ (4.4 Å). This suggests that the liquid crystalline phase formed by AzoPR-6 is columnar nematic phase [38]. Interestingly, when the spacer length increases to 11, another three obvious peaks in higher angular region appear. It is considered that the ordered liquid crystalline domains are formed by the mesogens on the PR besides the columnar nematic phase of the whole molecule, and these three peaks in higher angle region can be indexed with (110), (200), and (210)

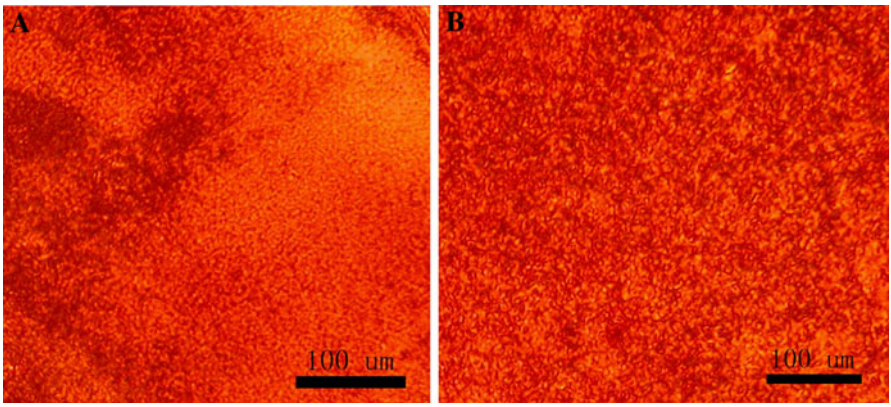

Fig. 6 Polarizing optical micrograph of AzoPR-6 (**a**) and AzoPR-11 (**b**) at 120 °C

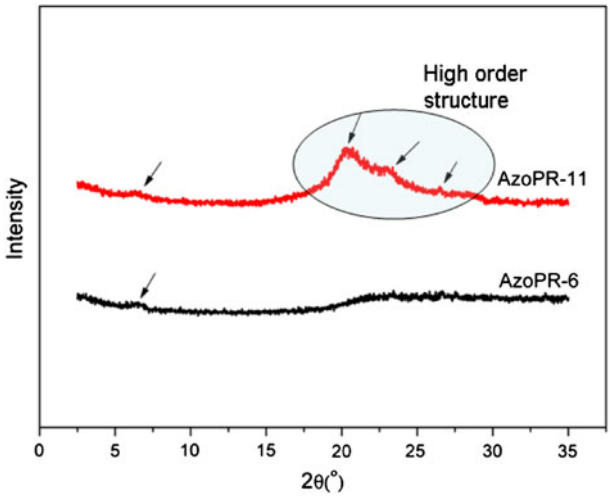

Fig. 7 WAXD patterns of AzoPR-6 and AzoPR-11 at 120 °C

according to an orthorhombic structure, indicating that the domains constructed by azobenzene mesogen can form high-order structures [39]. It can be found that the size of the columnar formed by the main chain of AzoPR-11 is approximately equal to the external cavity diameter of the α-CD, which implies that the mesogens are ordered arranged between the CD and located around the PR. The molecular model of AzoPR-11 is showed in Fig. 1. The trend that the liquid crystalline phase developed better with the increase of spacer length is ascribed to the fact that the interaction between the motions of pendants and the segmental motion of the backbone is decoupled with the increase of spacer length [36]. Unfortunately, it is that we can not obtain the accurate structure of the phase at higher temperature for AzoPR-11, because the covalent bond of CD starts to break after the endothermic transition from DSC data.

Conclusion

A series of liquid crystalline PRs containing azobenzene mesogenic moieties with different spacer length were successfully synthesized. PR was first prepared using α-CD, poly(ethylene glycol) (Mw = 8000) and 3,5-dimethylphenol end groups, afterward, AzoPR was obtained from the PR and azobenzene mesogens through esterification. The chemical structures of the intermediates and polymers were confirmed by combined characterization techniques. The phase structures and transitions of the polymers were investigated by DSC, POM, and WAXD. The experimental results suggested that AzoPR-2 and AzoPR-4 failed to show the liquid crystalline behavior, and AzoPR-6 shows the columnar nematic phase. However, when the spacer length increases to 11, the columnar nematic phase was formed; meanwhile, the liquid crystalline domains with high-order structure were developed by azobenzene mesogens.

Acknowledgments This research was financially supported by the National Nature Science Foundation of China (20874082), the Scientific Research Fund of Hunan Provincial Education Department (06A068), the Key Project of Chinese Ministry of Education for Science and Technology (NO. 207075) and the New Century Excellent Talents in University (NCET-05-0707).

References

1. Blumstein A (1985) Polymeric liquid crystals. Plenum Press, New York
2. Kondo M, Yu Y, Ikeda T (2006) How does the initial alignment of mesogens affect the photoinduced bending behavior of liquid-crystalline elastomers? Angew Chem Int Ed 45(9):1378–1382
3. Ikeda T, Nakano M, Yu Y, Tsutsumi O, Kanazawa A (2003) Anisotropic bending and unbending behavior of azobenzene liquid-crystalline gels by light exposure. Adv Mater 15(3):201–205
4. Tong X, Wang G, Zhao Y (2006) Photochemical phase transition versus photochemical phase separation. J Am Chem Soc 128(27):8746–8747
5. Verploegen E, Soulages J, Kozberg M, Zhang T, McKinley G, Hammond P (2009) Reversible switching of the shear modulus of photoresponsive liquid-crystalline polymers. Angew Chem Int Ed 48(19):3494–3498
6. Strand PO, Ramanujam PS, Hvilsted S, Bak KL, Sauer SPA (2000) Ab initio calculation of the electronic spectrum of azobenzene dyes and its impact on the design of optical data storage materials. J Am Chem Soc 122(14):3482–3487
7. Wang WY, Wang MZ (2007) Effect of α-cyclodextrin on the photoisomerization of azobenzene functionalized hydroxypropyl methylcellulose in aqueous solution. Polym Bull 59:537–544
8. Kumar GS, Neckers DC (1989) Photochemistry of azobenzene-containing polymers. Chem Rev 89(8):1915–1925
9. Yang YK, Wang XT, Liu L, Xie XL, Yang ZF, Li RKY, Mai YW (2007) Structure and photoresponsive behaviors of multiwalled carbon nanotubes grafted by polyurethanes containing azobenzene side chains. J Phys Chem C 111(30):11231–11239
10. Harada A (2001) Cyclodextrin-based molecular machines. Acc Chem Res 34(6):456–464
11. Liu Y, Yu ZL, Zhang YM, Guo DS, Liu YP (2008) Supramolecular architectures of β-cyclodextrin-modified chitosan and pyrene derivatives mediated by carbon nanotubes and their DNA condensation. J Am Chem Soc 130(31):10431–10439
12. Oddy FE, Brovelli S, Stone MT, Klotz EJF, Cacialli F, Anderson HL (2009) Influence of cyclodextrin size on fluorescence quenching in conjugated polyrotaxanes by methyl viologen in aqueous solution. J Mater Chem 19(18):2846–2852
13. Ramirez HL, Valdivia A, Cao R, Fragoso A, Labandeira JJT, Baños M, Villalonga R (2007) Preparation of β-cyclodextrin-dextran polymers and their use as supramolecular carrier systems for naproxen. Polym Bull 59:597–605

14. Li C, Isshiki N, Saito H, Kohno K, Toyota A (2009) The influence of side chains on formation of inclusion complexes prepared with polyolefin and cyclodextrins. Polym Bull 63:779–788
15. Huang FH, Gibson HW (2005) Polypseudorotaxanes and polyrotaxanes. Prog Polym Sci 30(10): 982–1018
16. Kidowaki M, Nakajima T, Araki J, Inomata A, Ishibashi H, Ito K (2007) Novel liquid crystalline polyrotaxane with movable mesogenic side chains. Macromolecules 40(19):6859–6862
17. Nepogodiev SA, Stoddart JF (1998) Cyclodextrin-based catenanes and rotaxanes. Chem Rev 98(5):1959–1976
18. Zhao T, Beckham HW (2003) Direct synthesis of cyclodextrin-rotaxanated poly(ethylene glycol)s and their self-diffusion behavior in dilute solution. Macromolecules 36(26):9859–9865
19. Kidowaki M, Zhao C, Kataoka T, Ito K (2006) Thermoreversible sol–gel transition of an aqueous solution of polyrotaxane composed of highly methylated α-cyclodextrin and polyethylene glycol. Chem Commun 39:4102–4103
20. Liu Y, Yang YW, Chen Y, Zou HX (2005) Polyrotaxane with cyclodextrins as stoppers and its assembly behavior. Macromolecules 38(13):5838–5840
21. Wenz G, Han BH, Müller A (2006) Cyclodextrin rotaxanes and polyrotaxanes. Chem Rev 106(3):782–817
22. Ooya T, Eguchi M, Yui N (2003) Supramolecular design for multivalent interaction: maltose mobility along polyrotaxane enhanced binding with concanavalin A. J Am Chem Soc 125(43): 13016–13017
23. Harada A, Li J, Kamachi M (1994) Preparation and characterization of a polyrotaxane consisting of monodisperse poly(ethylene glycol) and α-cyclodextrins. J Am Chem Soc 116(8):3192–3196
24. Jarroux N, Guégan P, Cheradame H, Auvray L (2005) High conversion synthesis of pyrene end functionalized polyrotaxane based on poly(ethylene oxide) and α-cyclodextrins. J Phys Chem B 109(50):23816–23822
25. Harada A, Li J, Kamachi M (1993) Synthesis of a tubular polymer from threaded cyclodextrins. Nature 364:516–518
26. Shimomura T, Akai T, Abe T, Ito K (2002) Atomic force microscopy observation of insulated molecular wire formed by conducting polymer and molecular nanotube. J Chem Phys 116(5):1753–1756
27. Taylor PN, O'Connell MJ, McNeill LA, Hall MJ, Aplin RT, Anderson HL (2000) Insulated molecular wires: synthesis of conjugated polyrotaxanes by Suzuki coupling in water. Angew Chem Int Ed 39(19):3456–3460
28. Ooya T, Arizono K, Yui N (2000) Synthesis and characterization of an oligopeptide-terminated polyrotaxane as a drug carrier. Polym Adv Technol 11(8–12):642–651
29. Yui N, Ooya T (2006) Molecular mobility of interlocked structures exploiting new functions of advanced biomaterials. Chem Eur J 12(26):6730–6737
30. Okumura Y, Ito K (2001) The polyrotaxane gel: a topological gel by figure-of-eight cross-links. Adv Mater 13(7):485–487
31. Raymo FM, Stoddart JF (1999) Interlocked macromolecules. Chem Rev 99(7):1643–1664
32. Cui YJ, Wang MQ, Chen LJ, Qian GD (2005) Synthesis and characterization of an alkoxysilane dye for nonlinear optical applications. Dyes Pigments 65(1):61–66
33. Cormack PAG, Moore BD, Sherrington DC (1997) Monodisperse liquid crystalline peptides. J Mater Chem 7(10):1977–1983
34. Araki J, Ito K (2006) New solvent for polyrotaxane. I. Dimethylacetamide/lithium chloride (DMAc/LiCl) system for modification of polyrotaxane. J Polym Sci Part A Polym Chem 44(1):532–538
35. Ni B, Wang XZ, Yu HG, Zhang XF, Zhang HL, Wong WY (2008) Synthesis and characterization of a novel diblock copolymer with a polyrotoxane block. Polym Bull 61(1):53–62
36. Cha SW, Jin JI, Kim DC, Zin WC (2001) Combined type liquid crystalline poly(oxy-1, 4-phenyleneoxyterephthaloyl)s bearing cholesterol pendants attached through polymethylene spacers. Macromolecules 34(15):5342–5348
37. Huang B, Ge JJ, Li YH, Hou HQ (2007) Aliphatic acid esters of (2-hydroxypropyl) cellulosed effect of side chain length on properties of cholesteric liquid crystals. Polymer 48(1):264–269
38. Ye C, Zhang HL, Huang Y, Chen EQ, Lu YL, Shen DY, Wan XH, Shen ZH, Cheng SZD, Zhou QF (2004) Molecular weight dependence of phase structures and transitions of mesogen-jacketed liquid crystalline polymers based on 2-vinylterephthalic acids. Macromolecules 37(19):7188–7196
39. Nieuwhof RP, Marcelis ATM, Sudhölter EJR, Picken SJ, Jeu WHD (1999) Side-chain liquid-crystalline polymers from the alternating copolymerization of maleic anhydride and 1-olefins carrying biphenyl mesogens. Macromolecules 32(5):1398–1406